Supplemental Data

Supplementary figure - graphical abstract

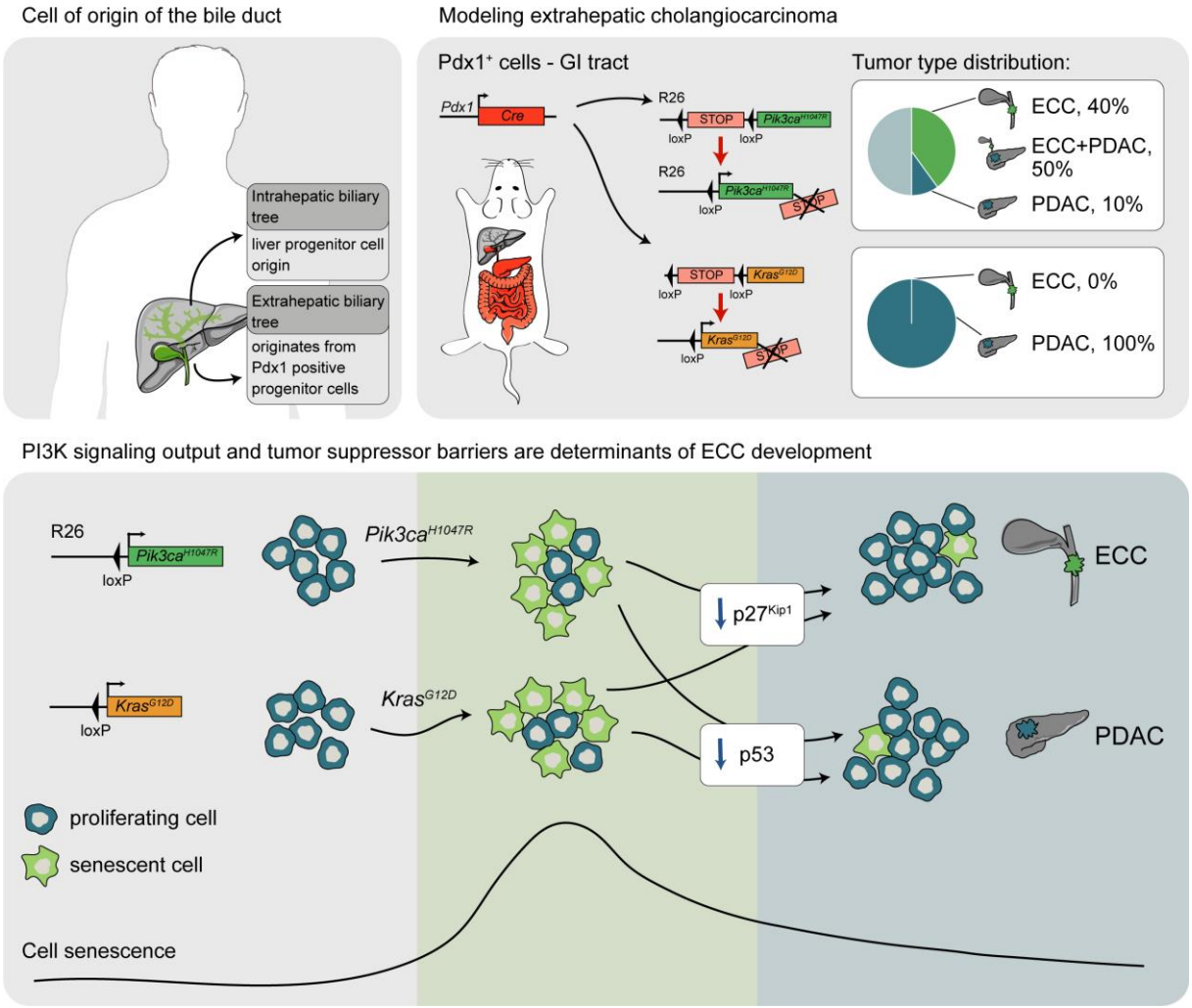

Graphical Abstract. Schematic overview of the background of the study, the novel genetically engineered mouse models of extrahepatic cholangiocarcinoma (ECC), and the context specific role of oncogenic PI3K and Kras signaling for ECC and pancreatic ductal adenocarcinoma (PDAC) formation.

Supplementary figure - S1

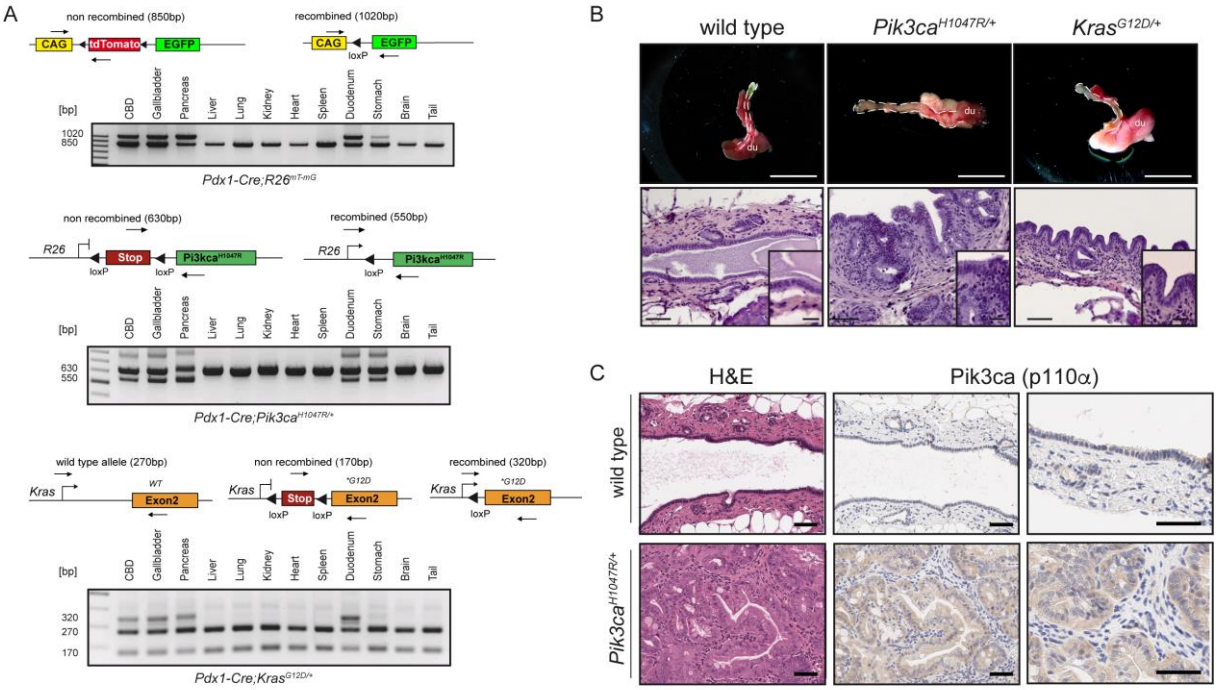

Supplementary Figure S1: Constitutive activation of the PI3K-signalling pathway induces premalignant biliary intraepithelial neoplasia (BilIN). (A) Genotyping strategy (upper panel schematics) and genotyping PCR (lower panel gel pictures) to analyze tissue-specific recombination of the *R26$^{mT\text{-}mG}$*, *LSL-Pik3ca^{H1047R}* and *LSL-Kras^{G12D}* alleles in *Pdx1-Cre;R26$^{mT\text{-}mG}$*, *Pdx1-Cre;LSL-Pik3ca$^{H1047R/+}$* and *Pdx1-Cre;LSL-Kras$^{G12D/+}$* mice, respectively (from top to bottom). Sizes of non-recombined mutant, recombined mutant and for *LSL-Kras^{G12D}* wild type PCR products are indicated. CBD, common bile duct. (B) Upper panel: Representative macroscopic images of the common bile duct (outlined by a white dashed line) of 6-months-old wildtype, *Pdx1-Cre;LSL-Pik3ca$^{H1047R/+}$* and *Pdx1-Cre;LSL-Kras$^{G12D/+}$* mice. du, duodenum. Lower panel: Representative H&E stainings of the common bile duct of the same animals. Scale bars, 1 cm for macroscopic images, 50 µm for micrographs, 20 µm for insets. (C) Representative H&E stainings and immunohistochemical analysis of Pik3ca (p110α) expression in the biliary epithelium of the common bile duct of wild type control (upper panel) and *Pdx1-Cre;LSL-Pik3ca$^{H1047R/+}$* (lower panel) mouse. Scale bars, 50 µm.

Supplementary figure - S2

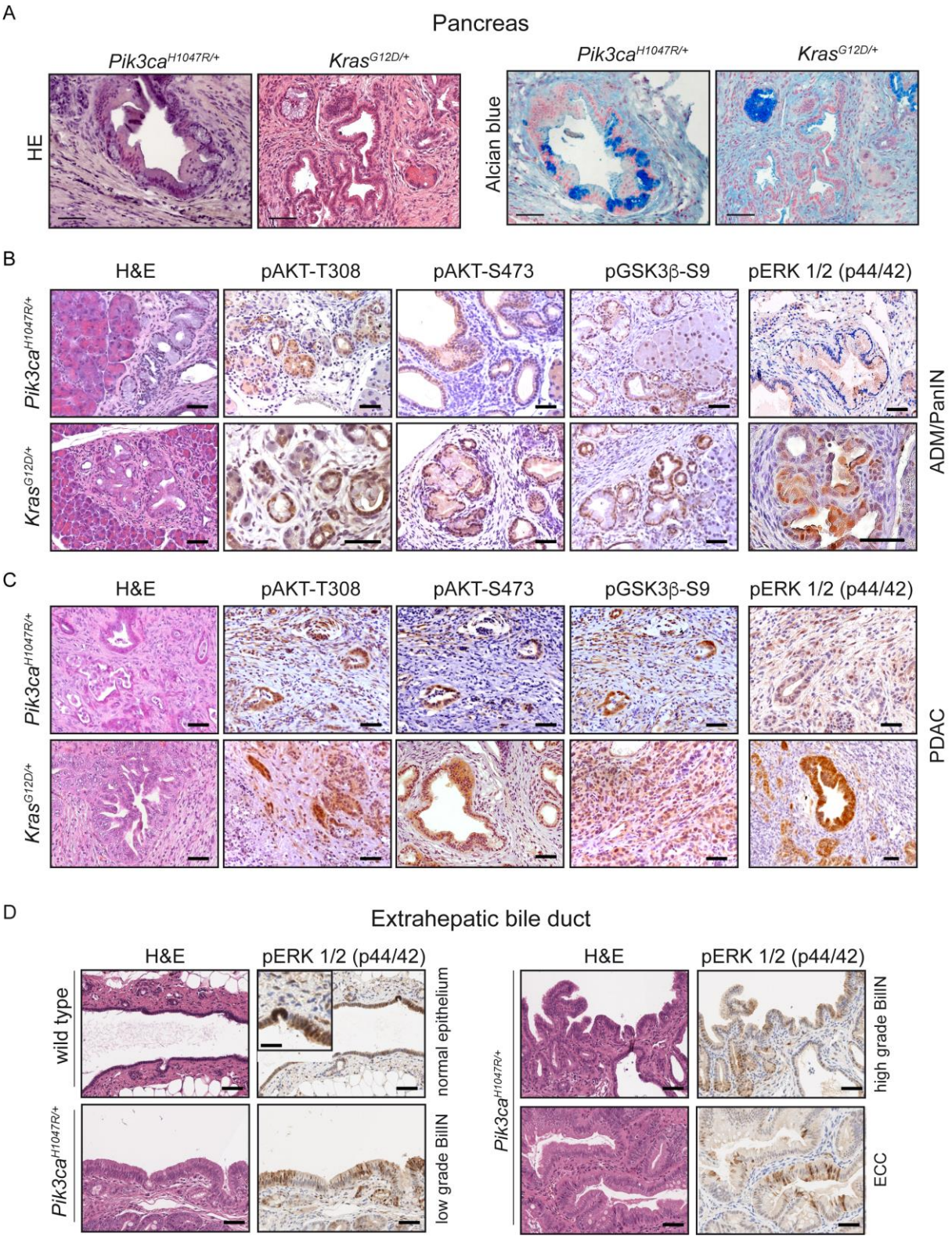

Supplementary Figure S2: Activation of *Pik3ca*$^{H1047R/+}$ and Kras$^{G12D/+}$ in the *Pdx1-Cre* lineage induces ADM, PanIN and PDAC. (A) Representative H&E and Alcian blue stained sections of the pancreas with acinar-ductal metaplasia (ADM) and low-grade pancreatic intraepithelial neoplasia (PanIN) of *Pdx1-Cre;LSL-Pik3ca*$^{H1047R/+}$ and

Pdx1-Cre;LSL-Kras$^{G12D/+}$ mice. (B) H&E staining and immunohistochemical analysis of PI3K/AKT and MAPK pathway activation in ADM and PanIN lesions of *Pdx1-Cre;LSL-Pik3ca*$^{H1047R/+}$ and *Pdx1-Cre;LSL-Kras*$^{G12D/+}$ mice. (C) H&E staining and immunohistochemical analysis of PI3K/AKT and MAPK pathway activation in PDAC of *Pdx1-Cre;LSL-Pik3ca*$^{H1047R/+}$ and *Pdx1-Cre;LSL-Kras*$^{G12D/+}$ mice. (D) Representative H&E stainings and immunohistochemical analysis of MAPK pathway activation in the biliary epithelium of the common bile duct of wild type control and *Pdx1-Cre;LSL-Pik3ca*$^{H1047R/+}$ (lower panel) mouse. Scale bars, 50 μm for micrographs and 20 μm for insets.

Supplementary figure - S3

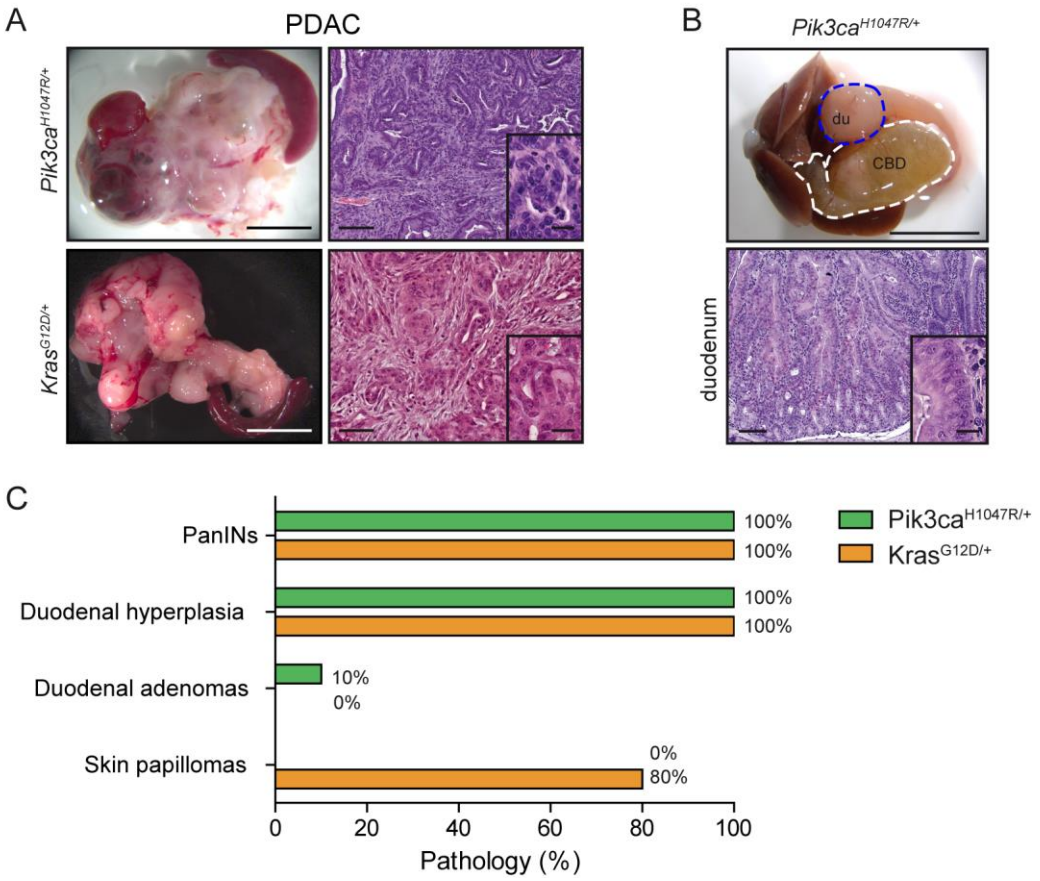

Supplementary Figure S3: Pathologies induced by expression of oncogenic Pik3ca^{H1047R} or Kras^{G12D} in the pancreas, duodenum and skin (A) Representative macroscopic (left panel) and microscopic H&E stained (right panel) images of pancreatic ductal adenocarcinoma (PDAC) of *Pdx1-Cre;LSL-Pik3ca$^{H1047R/+}$* and *Pdx1-Cre;LSL-Kras$^{G12D/+}$* mice. (B) Representative macroscopic image of a dilated common bile duct (CBD; outlined by a white dashed line) and an adenoma in the duodenum (du; blue dashed line) of a *Pdx1-Cre;LSL-Pik3ca$^{H1047R/+}$* mouse (upper panel). Microscopic picture of H&E stained adenoma in the duodenum of *Pdx1-Cre;LSL-Pik3ca$^{H1047R/+}$* mouse (lower panel). (C) Occurrence of pathologies in *Pdx1-Cre* expressing tissues from *Pdx1-Cre;LSL-Pik3ca$^{H1047R/+}$* and *Pdx1-Cre;LSL-Kras$^{G12D/+}$* mice. Scale bars, 1 cm for macroscopic images, 50 µm for micrographs, 20 µm for insets.

Supplementary figure - S4

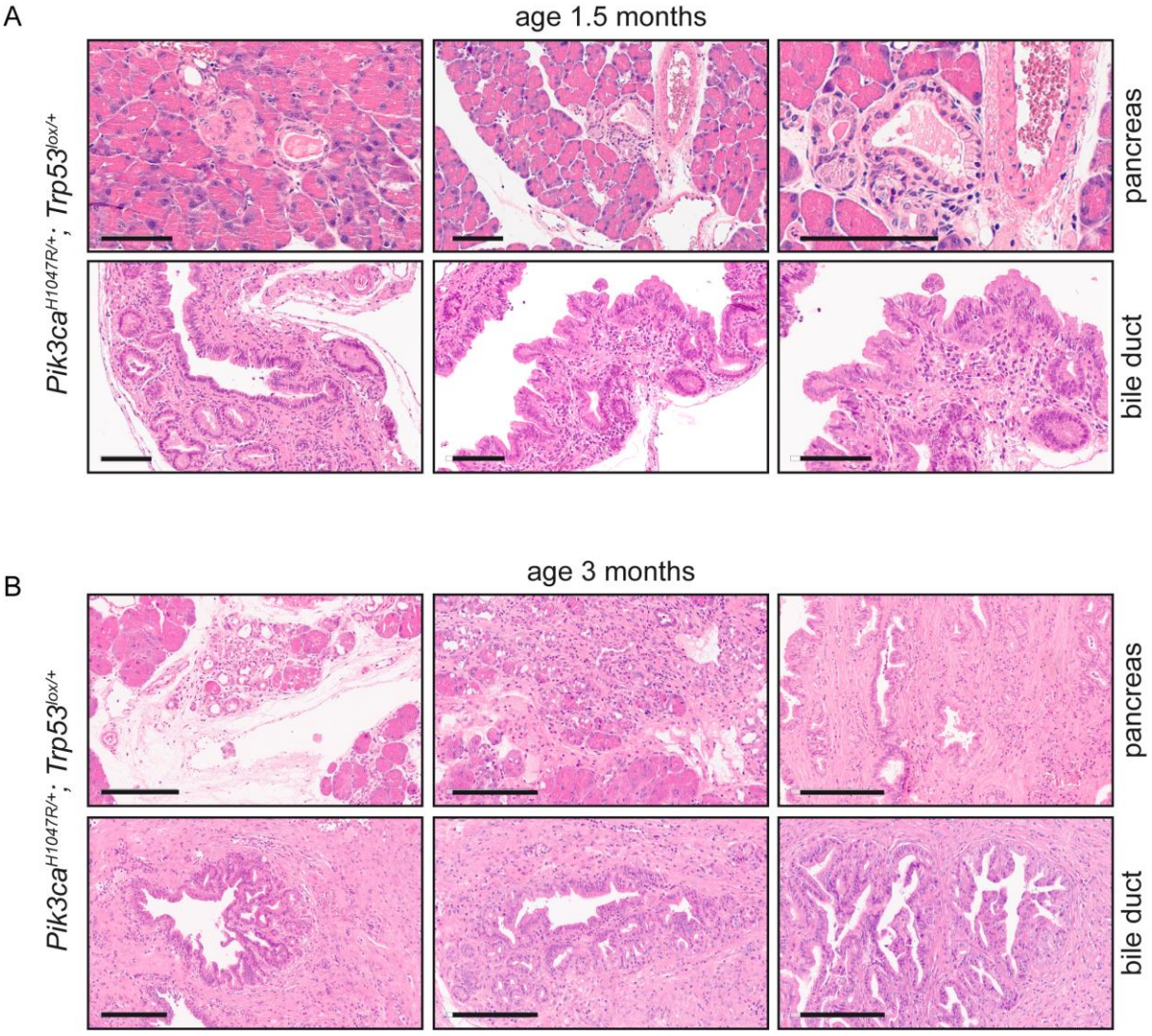

Supplementary Figure S4: BilIN/PanIN development and ECC/PDAC occurrence in *Trp53* mutant *Pdx1-Cre;LSL-Pik3ca$^{H1047R/+}$* animals. (A) Representative microscopic images of H&E stained sections of the pancreas (upper panel) and the extrahepatic bile duct (lower panel) of 1,5 month old *Pdx1-Cre;LSL-Pik3ca$^{H1047R/+}$*;*Trp53$^{lox/+}$* mice. Scale bars, 100 µm. (B) Representative microscopic images of H&E stained sections of the pancreas (upper panel) and the extrahepatic bile duct (lower panel) of 3 months old *Pdx1-Cre;LSL-Pik3ca$^{H1047R/+}$*;*Trp53$^{lox/+}$* mouse. Scale bars, 200 µm.

Supplementary figure - S5

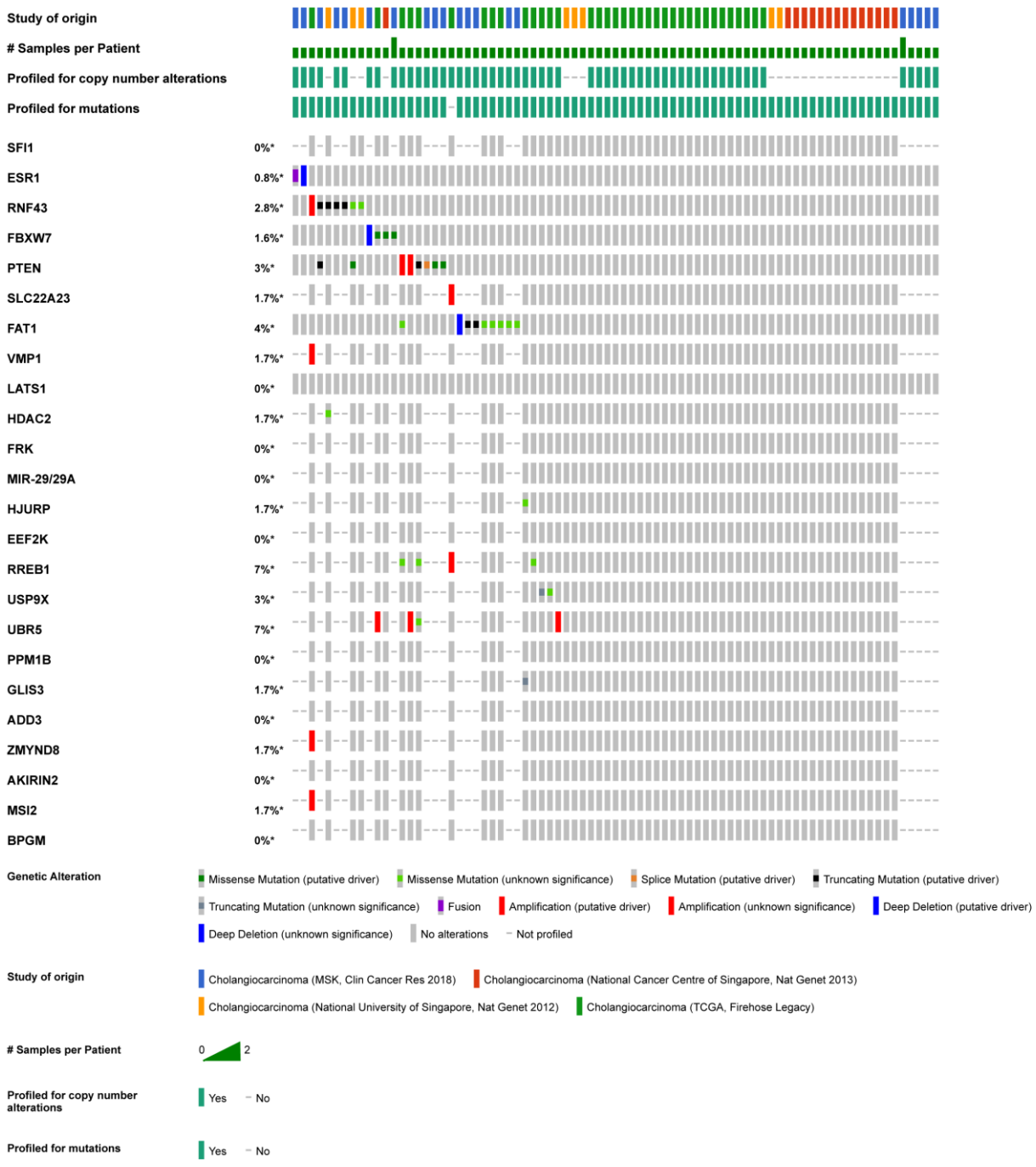

Supplementary Figure S5: Comparison of the top 24 Common Insertion Sites (CIS) of the *piggyBac* transposon mutagenesis screen with recurrent genetic aberrations in human bile duct cancer. The analysis was carried out on cBioportal (http://www.cbioportal.org/).

Supplementary figure - S6

Scheme of hits identified in the extrahepatic biliary tract by a *piggyBac* transposon mutagenesis screen

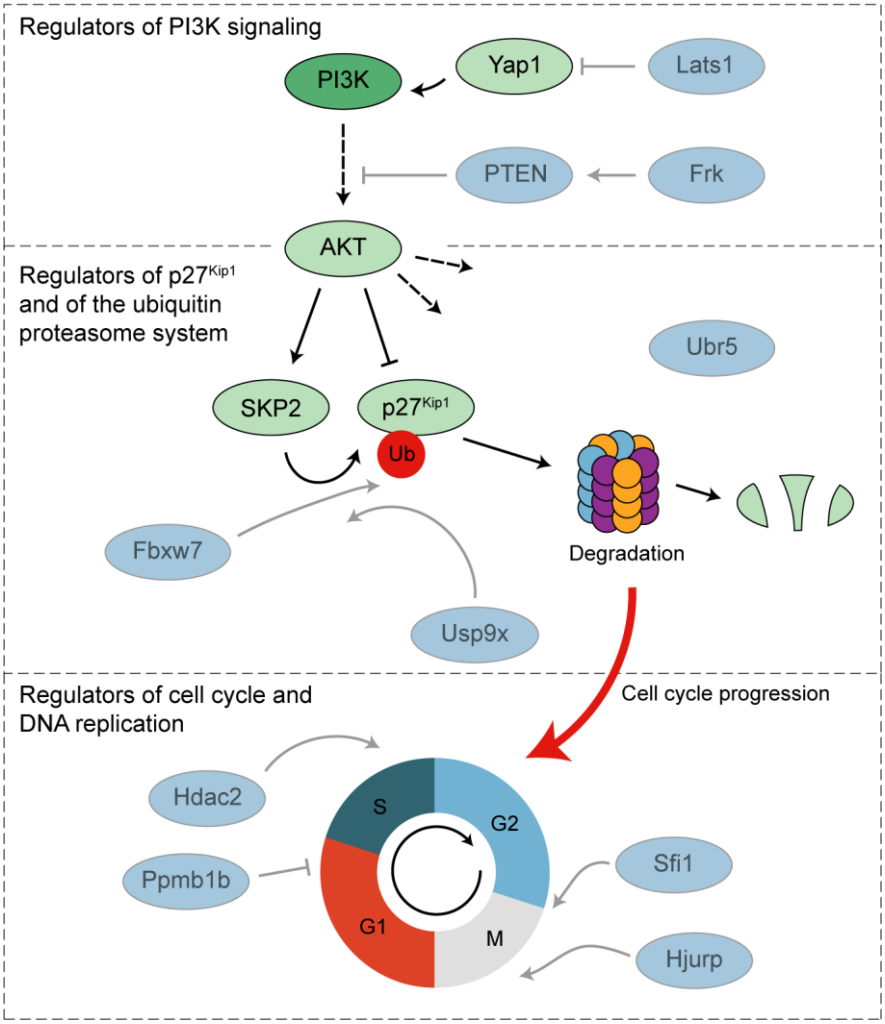

Supplementary Figure S6: Schematic of the most frequent Common Insertion Sites (CIS) of the *piggyBac* transposon mutagenesis screen. The identified top CIS, here represented in blue, are PI3K signaling regulators, direct and indirect modulators of $p27^{Kip1}$ protein abundance and regulators of cell cycle and DNA replication.

Supplementary figure - S7

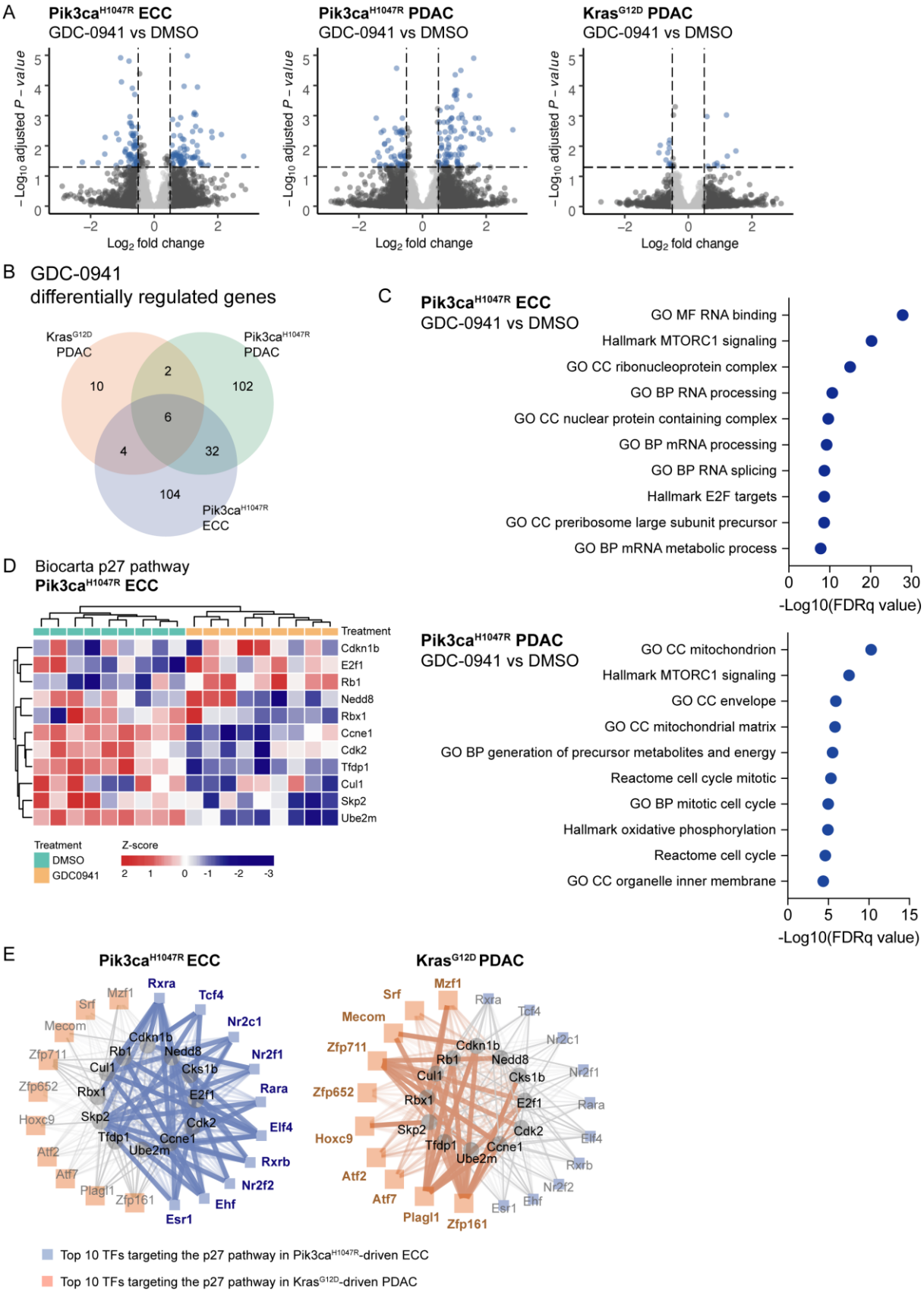

Supplementary Figure S7: RNA-seq analysis of primary low-passaged ECC and PDAC cell cultures isolated from Pik3ca^{H1047R}- and Kras^{G12D}-driven mouse

models. (A) ECC and PDAC cell cultures (n=3 cell cultures per tumor type) were treated with the PI3K inhibitor GDC-0941 (1µM) or vehicle (DMSO) for 48 h in triplicate and analyzed by RNA-seq. Volcano plot displaying the differences in gene expression for DMSO treated cells relative to GDC-0941 of the different genotypes and tumor types. Significantly differentially expressed genes (false discovery rate (FDR)-corrected P ≤ 0.05) are highlighted in blue, with the dotted lines representing the boundary for identification of up- or down-regulated genes. The left panel shows the differentially expressed genes for $Pik3ca^{H1047R}$-driven ECC, the middle panel for $Pik3ca^{H1047R}$-driven PDAC and the right panel for $Kras^{G12D}$-driven PDAC. (B) Venn diagram showing the overlap of the differentially expressed genes (FDR-corrected P ≤ 0.05; absolute fold change >0.5) upon GDC-0941 treatment across tumor entities. (C) Top 10 enriched gene sets ranked based on -log10(FDR)q value. The analysis was performed using the RNA-seq data of vehicle and GDC-0941 treated $Pik3ca^{H1047R}$-driven ECC (upper panel) and $Pik3ca^{H1047R}$-driven PDAC (lower panel) cells, respectively. The enrichment of the shown over-representation analysis was performed using gene sets from the H, C2 and C5 collections from MSigDB v7.1. (D) Heatmap showing the expression of the genes of the Biocarta p27 pathway gene set in $Pik3ca^{H1047R}$-driven ECC, for DMSO and GDC-0941 treated cells. The color code indicates the Z score. (E) Regulatory network analysis showing the top 10 transcription factors targeting the $p27^{Kip1}$ pathway in $Pik3ca^{H1047R}$-driven ECC (left) and $Kras^{G12D}$-driven PDAC (right). The $p27^{Kip1}$ core pathway genes shown in the center of the circle were obtained from the Biocarta p27 pathway gene set. The TF were selected as the most differentially regulating ones after inferring the regulatory networks using PANDA. Interactions of TFs with p27 core pathway genes are marked by lines in different colors (blue, interactions in $Pik3ca^{H1047R}$-driven ECC; orange, interactions in $Kras^{G12D}$-driven PDAC; grey, non-significant interactions). The thickness of the lines represent the strength of interaction. Cdkn1b, $p27^{Kip1}$.

Supplementary figure - S8

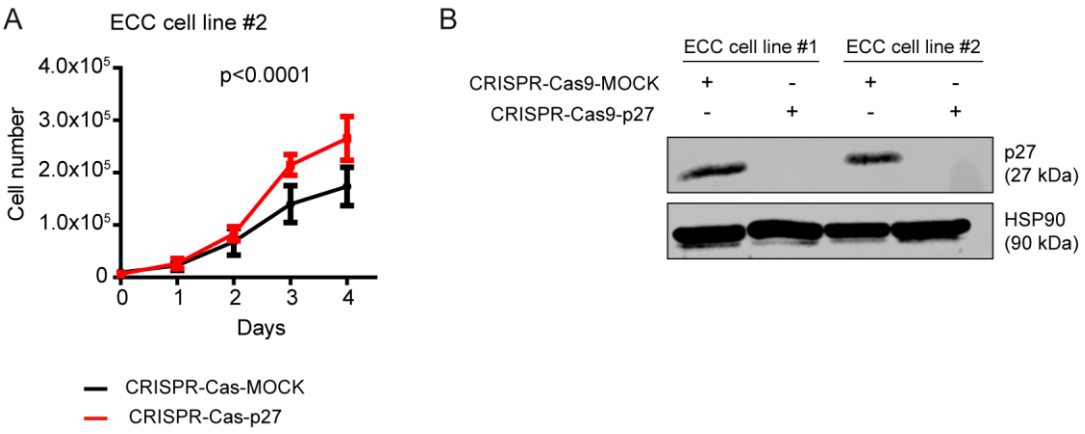

Supplementary Figure S8: p27^{Kip1} is a context-specific roadblock for Kras-induced ECC formation. (A) Proliferation analysis of a primary murine ECC cell line #2 from a *Pdx1-Cre;LSL-Pik3ca$^{H1047R/+}$* mouse after CRISPR-Cas9 mediated deletion of *Cdkn1b* (*p27^{Kip1}*). Cells were transfected with either Cas9 expression vectors containing sgRNAs targeting *Cdkn1b* (CRISPR-Cas-p27) or a MOCK Cas9 nickase expression vector containing a sgRNA targeting *Cdkn1b* (CRISPR-Cas-MOCK). Proliferation was assessed by cell counting on 5 consecutive days in triplicate (n=4, mean ± s.d., p<0.0001, 2-way ANOVA). (B) Immunoblot analysis of p27^{Kip1} expression of CRISPR-Cas9-sgRNA-p27^{Kip1} or CRISPR-Cas9-sgRNA-MOCK transfected ECC cell lines used in the viability assay (see also Figure 7G). Hsp90α/β was used as loading control on the same blot.

Supplementary Methods

Oligonucleotides for generation of sgRNAs targeting *Cdkn1b*

Oligonucleotide	Sequence (5'-3')
Cdkn1b-sgRNA1-for	CACCGTGCAGAAATCTCTTCGGCC
Cdkn1b-sgRNA1-rev	AAACGGCCGAAGAGATTTCTGCAC
Cdkn1b-sgRNA2-for	CACCGTTTCAGAATCATAAGCCCC
Cdkn1b-sgRNA2-rev	AAACGGGGCTTATGATTCTGAAAC

qRT-PCR Primers

Species	Transcript	Primer name	Sequence (5´ - 3´)
mouse	$p27^{Kip1}$	$p27^{Kip1}$ forward	GTGGACCAAATGCCTGACTC
		$p27^{Kip1}$ reverse	TCTGTTCTGTTGGCCCTTTT
mouse	cyclophilin	cyclophilin forward	ATGGTCAACCCCACCGTGT
		cyclophilin reverse	TTCTTGCTGTCTTTGGAACTTTGTC

Primers for genotyping and recombination PCRs

PCR	Primer	Sequence (5'-3')
LSL-PIK3CA	$PI3K^{H1047R}$ MUT forward	TGAATAGTTAATTGGAGCGGCCGCAATA
	$PI3K^{H1047R}$ MUT reverse	AAATAGCCGCAGGTCACAAAGTCTCCG
Rosa26	R26 common forward	AAAGTCGCTCTGAGTTGTTAT
	R26 MUT reverse	GCGAAGAGTTTGTCCTCAACC

	R26 WT reverse	GGAGCGGGAGAAATGGATATG
Pdx1-Cre	Pdx1-Cre forward	GCTCATTGGGAGCGGTTTTG
	Cre reverse	ACATCTTCAGGTTCTGCGGG
	Control reverse	CACGTGGTTTACCCTGGAGC
$R26^{tdTo}$	tdTomato forward	CAAGGGAGAGGAGGTCATCAAAG
	tdTomato reverse	GCTTGGTGTCCACGTAGTAGTAGC
$R26^{mT/mG}$	R26 common forward	AAAGTCGCTCTGAGTTGTTAT
	R26 mT/mG reverse	GTACTTGGCATATGATACACTTGATGTAC
	R26 WT reverse	GGAGCGGGAGAAATGGATATG
LSL-Kras (+del)	Kras common forward	CACCAGCTTCGGCTTCCTATT
	Kras WT/del reverse	AGCTAATGGCTCTCAAAGGAATGTA
	$Kras^{G12D}$ MUT reverse	CCATGGCTTGAGTAAGTCTGC
$p53^{f}$	p53 floxed forward	CACAAAAAACAGGTTAAACCCAGC
	p53 floxed reverse	GCACCTTTGATCCCAGCACATA
p27 knock-out	p27 common forward	TGGAACCCTGTGCCATCTCTAT
	p27 knock-out reverse	CCTTCTATGGCCTTCTTGACG
p27 wild type	p27 common forward	TGGAACCCTGTGCCATCTCTAT
	p27 WT reverse	GAGCAGACGCCCAAGAAGC
PIK3CA del	$PI3K^{H1047R}$ del forward	CAGTAGTCCAGGGTTTCCTTGATG
	$PI3K^{H1047R}$ MUT forward	TGAATAGTTAATTGGAGCGGCCGCAATA
	$PI3K^{H1047R}$ MUT reverse	AAATAGCCGCAGGTCACAAAGTCTCCG

$R26^{mT/mG}$ del	R26 mT/mG common forward	GTTCGGCTTCTGGCGTGT
	tdTomato reverse	GCTTGGTGTCCACGTAGTAGTAGC
	EGFP reverse	CCATGTGATCGCGCTTCTCGT